A Fundamental Investigation of Premixed Hydrogen Oxy-combustion in Carbon Dioxide

Md Nayer Nasim[1], Behlol Nawaz[1], Shubhra Kanti Das[1], Amina SubLaban[1] and J. Hunter Mack[1]

[1] Department of Mechanical Engineering, University of Massachusetts Lowell, 1 University Avenue, Lowell, MA, USA.

E-mail: John_Mack@uml.edu
Telephone: +(1) 978 934 5766

Abstract. Hydrogen (H_2) is increasingly viewed as an attractive carbon-free fuel due to its potential compatibility with the existing transportation and conversion infrastructure. However, one of the major challenges facing large-scale deployment is the fundamentally different combustion properties it has in comparison to commonplace hydrocarbon fuels such as natural gas. For example, the laminar burning velocity (LBV) of a combustible mixture has a direct impact on how it can be used in internal combustion engine or gas turbines; the LBV of hydrogen is over 7 times greater than that of natural gas when combusted in air. Carbon dioxide (CO_2) can be used as a working fluid, as opposed to nitrogen (in air), to reduce the flame speed of hydrogen combustion. A mixture of hydrogen, oxygen, and carbon dioxide as a working fluid can provide LBVs comparable to natural gas in air, which potentially enables existing conversion architectures. Furthermore, by replacing nitrogen (N_2) with CO_2 in the mixture, NO_x emissions are avoided and opportunities for carbon sequestration or closed-cycle processes are possible. This study experimentally explores fundamental premixed oxy-combustion properties of H_2/CO_2 mixtures in a constant volume combustion chamber (CVCC) across a range of initial pressures (1, 1.5 and 2 bar) and equivalence ratios (0.4, 0.6, 0.8, 1). The spherically expanding flames are examined to determine the flame speed, LBV, and lower flammability limits (LFL) with respect to different CO_2 concentrations (40%, 60%, 65%). Furthermore, it was identified that the flame speed of the 65% CO_2 case at an equivalence ratio of 1 and initial pressure of 1 bar matches the closest with methane-air stoichiometric combustion.

Nomenclature

LBV	Laminar burning velocity
CVCC	Constant volume combustion chamber
FL	Flammability limit
P_i	Initial pressure
MIE	Minimum ignition energy

1. Introduction

The transportation sector requires approximately 5.6 × 1020 J of energy per year, primarily dependent on fossil fuels by consuming around 11 billion liters of fuel every day to power approximately 380 million commercial vehicles and 1.2 billion passenger cars worldwide [1-4]. Light-duty vehicles, especially gasoline-fueled passenger cars, supply 44% of global transport energy demand and gasoline-based spark-ignition engines power around 80% of the total passenger cars worldwide [5,6].

With the increasing energy demand and decarbonization technology transition, it is imperative to reduce the usage of fossil fuels by utilizing cleaner alternative fuels that can leverage the existing internal combustion engines and gas turbines to ensure efficient combustion with low anthropogenic carbon emission. Hydrogen is one of the cleanest fuels with lower minimum ignition energy (0.017 mJ) [7], lower volumetric energy density [8], higher diffusivity [9], and a wider flammability range (4–75 vol%) [10] in comparison to traditional alternative fuels. These intrinsic properties of hydrogen result in a highly energetic rapid/instantaneous burning and propagation velocity, which is ten times higher than methane [11] and poses challenges to a potential drop-in replacement strategy. One method to address the rapid combustion is to add inert gases that suppress the rapid combustion event. Depending on the dilutant type and dilutant ratio, a different predominant effect is observed during the combustion process [12-

14]. One of the critical metrics to quantify this difference is the laminar burning velocity (LBV), a key parameter in premixed combustion measured as the normal component of flame velocity relative to unburned gas. It contributes to understanding the mixture diffusivity, reactivity, and exothermicity [15-17]. Numerous experimental efforts demonstrated the effect of inert gas addition such as argon, helium, nitrogen, carbon di-oxide and water vapor on hydrogen premixed combustion [18, 13, 19]. Duan and Liu [20] investigated premixed laminar flame of a H_2-air mixture with diluted N_2+H_2O and concluded a 64.3% decrease in flame propagation velocity with a dilution ratio from 10-40% at an equivalence ratio of 1, an initial pressure of 0.1 MPa and an initial temperature of 393K. Morovatiyan et al. [21] utilized argon as a working fluid in a $H_2/O_2/N_2$ premixed flames for 0.2–0.6 bar initial pressure, 298 K initial temperature and a broad range of equivalence ratio (0.2–3.0) and concluded that with the increasing argon content in the mixture, the flame speed and burning velocity increased while extending the lean flammability limit. Wang et al [22] examined the flame characteristics under sub-atmospheric pressure and room temperature with a wide range of equivalence ratios of H_2/air pre-mixtures diluted with Ar, N_2, and CO_2. Their experiments indicated that maximum pressure rises, and deflagration index are primarily dependent on dilutant type, and fraction while CO_2 was mentioned as a most effective inert gas for decreasing the speed associated with flame front expansion followed by the N_2 and Argon. Zhang et al. [18] conducted a computational study in terms of the efficacy of combustion suppression for N_2, He, Ar, and CO_2 and indicated Ar < N_2 < He < CO_2 in terms of effectiveness. When CO_2 is mixed with H_2 for ignition, [23] additional energy is required to raise the mixture temperature compared to nitrogen due to the higher specific heat capacity [24]. Li. et al. [25] investigated laminar combustion characteristics of N_2/ H_2/air and CO_2/ H_2/air and summarized that CO_2 has a more substantial dilution effect than N_2 in reducing LBV owing to both chemical effect and thermal effect. Katsumi et al. [26] studied the effects of CO_2 and water vapor mixture on hydrogen/air premixed flames and concluded that the addition of CO_2 or H_2O advances the unstable motion of hydrogen flames, and the reason was explained by the increment of diffusive-thermal behaviors of the flames. One standard method to intake CO_2 or H_2O vapor into the engine cylinder is utilizing the exhaust gas recirculation [27,28]; however, different CO_2 reformer methodology is still under research which can be implemented and incorporated into the future mobile transportation system [29].

Considering all the above, using CO_2 as the working fluid has the potential to balance the high LBV and make the use of H_2 more compatible with existing systems. Furthermore, replacing nitrogen eliminates the potential NOx emissions and may be used with carbon sequestration and closed-loop cycles. This experimental work investigated premixed hydrogen oxy-combustion with CO_2 as a working fluid, varying equivalence ratios ranging from 0.6 to 1.0 under different initial pressure conditions. The experiments were carried out in an optically accessible constant volume combustion chamber and a z-type schlieren technique was utilized to capture the flame morphology and a dynamic pressure sensor to measure chamber pressure.

2. Methodology

Flame speed, laminar burning velocity (LBV), and the lower flammability limits (LFL) are calculated for hydrogen gas combustion under a matrix of experimental conditions of varying the percentage of CO_2 in the mixture (CO_2%), initial pressure (1.0 bar, 1.5 bar, 2.0 bar), and equivalence ratio (1.0, 0.8, 0.6). Figure 1 shows the experimental setup, including the constant volume combustion chamber (CVCC), gas tanks, pressure transducers, and Schlieren imaging used to acquire data for the analysis.

The stainless-steel CVCC has an internal diameter of 140 mm and a volume of 1.93 L. Two 127 mm thick quartz viewing windows are supported by flanges. Proper sealing of the chamber is required for filling the chamber with the gas mixtures, ensuring constant volume during combustion, and for sufficient vacuuming after combustion; therefore, a high temperature O-ring is planted between the quartz windows and flanges. In order to generate a spark ignition, two electrodes are inserted from symmetrically opposite sides of the chamber, leaving a 1.36 mm gap where the spark occurs. The spherically expanding flame is observed using the optically accessible CVCC and a Z-type Schlieren imaging setup. The optical system uses a halogen light source (FSI-1060-250, 250 watt) that passes through a pinhole, two condensing lenses, the CVCC itself, a knife edge, two concave mirrors (internal diameter of 152.4 nm, focal length of 1524 nm), and a complementary metal oxide semiconductor (CMOS) Edgertronic SC2+ camera. Figure 1 shows the route of light path starting at the halogen source and ending at the high-speed camera. Table 1 includes all the characteristics of the optical system in use.

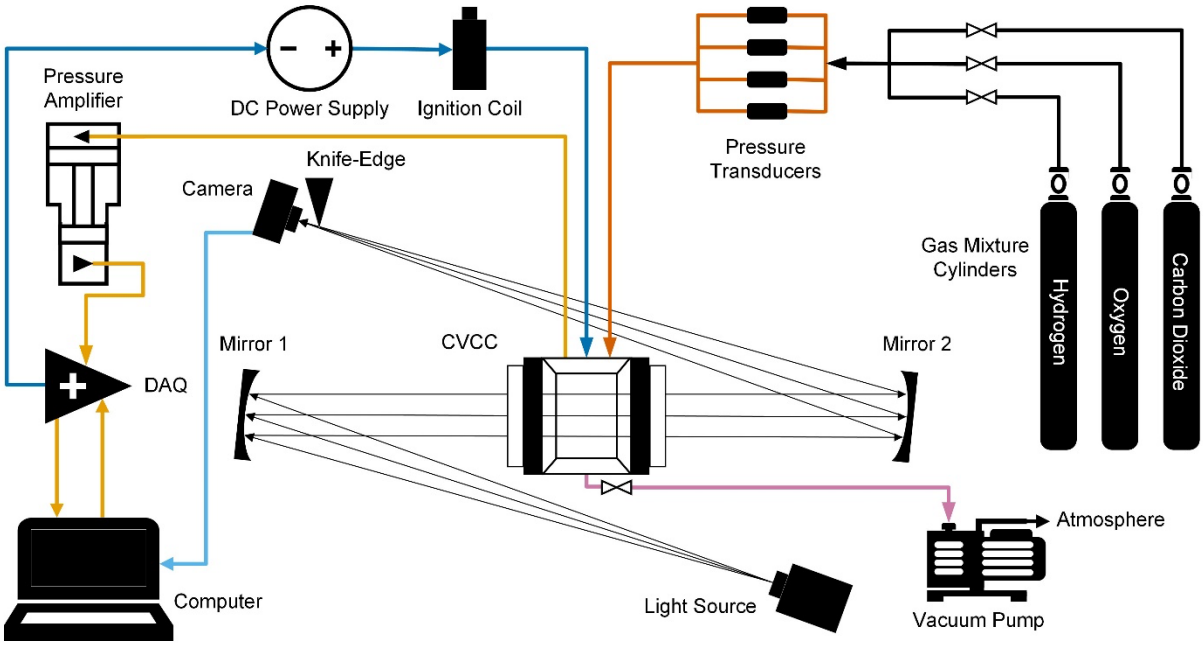

Figure 1: Schematic diagram of the experimental setup

Table 1. Optical System Configuration

Camera type	Complementary metal oxide semiconductor (CMOS)
Field of view	14 cm
Frame rate	8000 fps
Exposure	1/8500 seconds
Spatial resolution	4 mm/pixel

The start of a trial begins with vacuuming the CVCC and gas supply lines to <300 millitorrs to ensure the absence of undesired gases. The hydrogen gas, oxygen, and carbon dioxide are added to the chamber in ascending order of partial pressures. The gas supply lines are vacuumed in between the addition of each gas. Once all gases are loaded into the chamber, the mixture is allowed to mix for 3 minutes before spark. The spark is then triggered, and the data acquisition system records the image of the flame propagation, pressure, and time data. Each experimental condition, found within the experimental matrix, is repeated three times to guarantee repeatability and a >95% confidence level.

2.1 Flame Speed and Laminar Burning Velocity (LBV)

The images recorded using the Schlieren setup are digitally processed for flame speed calculations. Equation 1 is used:

$$S_b = \frac{dr_f}{dt} \tag{1}$$

where dr_f is the change of flame radius (cm) and dt is the change in time (s). The flame radii of interest are analyzed within upper and lower limits; the lower limit is set to 14 mm, or about 10x the distance of the 1.36 mm electrode gap, and the upper limit is set to 40 mm which is the maximum distance the flame can travel before making physical contact to the chamber walls. The laminar burning velocity is measured through two different methods. The first method uses the Schlieren images. This method is based on an experimental approach to calculate the flame speeds from Schlieren imaging. The images are converted into greyscale and then binarized to detect the edge of the expanding flame. Image processing and edge detection was performed with the image processing toolbox in MATLAB. The equivalent diameter of the propagating flame was calculated for each frame assuming the captured

region to be a complete circle. After identifying the region where the flame was expanding in a quasi-steady state, the instantaneous flame speed and stretch rate were calculated within that range for two consecutive images from the sequence. The flame stretch rate is defined as the time rate of the change of the flame surface area normalized by the area itself [30], as shown in Equation 2.

$$K = \frac{1}{A}\frac{dA}{dt} = \frac{2}{r_f}\frac{dr_f}{dt} = 2\frac{S_b}{r_f} \quad (2)$$

The unstretched flame speed was then measured by applying a linear fit to the stretch rate versus flame speed curve. The laminar burning velocity of the gas mixture was determined by multiplying the average unstretched flame speed with the expansion factor, i.e., density ratio of the burned and unburned gases which was determined by the free flame function in CANTERA for each of the mixture configurations tested. Hence, each experiment yielded a single value of laminar burning velocity and burned gas Markstein length.

The second method in which the LBV is calculated shows its correlation with the unburned gas temperature using a thermodynamic multi-shell model that relies on the experimental pressure data obtained during the flame propagation. Considering conservation of mass and energy, and employing ideal gas laws, the multi-shell model divides the chamber into different shells: the burned and unburned gas shells, which are divided by a negligibly thick flame front, and a third shell located between the wall of the chamber and the unburned gas shell. Further details regarding the fundamentals of the Metghalchi and Keck multi-shell model are expanded on in past literature [31] and more thorough mathematical details of converting pressure data to LBV are outlined in previous works [32]. Despite having instabilities on the flame surface, no self-acceleration was observed during the flame front propagation inside the CVCC. This allows us to use the multi-shell model for the laminar burning velocity calculations.

2.3 Flammability Limit (FL)

The FL of the hydrogen gas mixtures is determined by a trial-and-error approach that gradually alters conditions until the mixture does not ignite. For example, at a constant initial pressure, CO_2% was gradually increased in increments of 1% until the hydrogen gas ceases to ignite. In all experiments, the distance between the electrodes was always kept constant.

3. Result and Discussion

3.1 Flame morphology

Figure 2 and 3 illustrate the Schlieren images of spherically expanding flames inside the CVCC for H_2-O_2-CO_2 combustion at different initial pressures (1 bar and 2 bar, respectively) and fractions of CO_2 (40%, 60%, 65%) at stoichiometric conditions. These images give a qualitative validation to the assumption that increasing the CO_2 concentration in the mixture allows for the reduction of the flame speed for hydrogen oxy-combustion. From Figure 2, it can be seen that the spherically propagating flame takes only 3 ms to reach a radial value of 4.6 cm from the onset of ignition. The time to reach a similar radial value increases to 13.63 ms and 29.88 ms for the cases where CO_2 concentration was increased to be 60% and 65% respectively. Figure 4 exhibits a comparison of the flame speed between the 65% CO_2 case and methane-air stoichiometric combustion. It shows that the flame speed of hydrogen has become slower than that of methane-air combustion which took 18.63 ms to reach a radial value of 4.6 cm inside the CVCC.

Figure 3 shows another interesting in trend that, at 40% CO_2 conditions, the flame front propagates faster as the initial pressure is increased from standard pressure to an elevated pressure (2 bar). A similar trend was observed for hydrogen-air combustions by Ijima and Takeno [33]. However, as the percentage of CO_2 was increased above 40%, this trend changed and the flame speed started to decrease with increasing initial pressures. At this stage, the hydrogen oxy-combustion started showing characteristics similar to that of natural gas combustion, where the flame speed decreases with increasing initial pressures [32]. This can be attributed to the high thermal heat capacity of CO_2 compared to N_2 (~35 times greater), where the working fluid acts like a heat sink and decreases the net reaction rate, thereby reducing the flame speed. Increasing the CO_2 concentration of the mixture lowers the mixture's ability to overcome the activation energy for several reactions relevant to ignition [34]. Upon increasing the concentration of CO_2, the flame speed is lower than that of methane-air stoichiometric combustion.

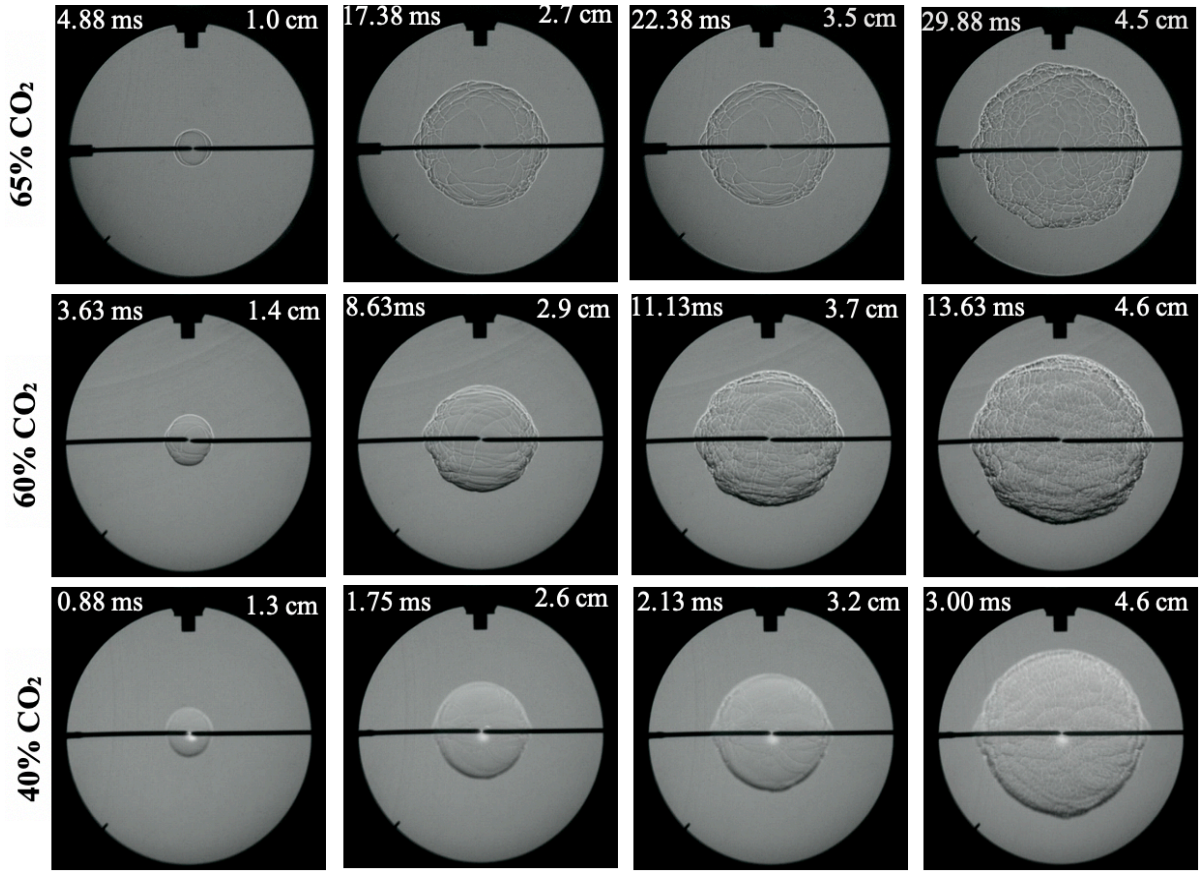

Figure 2: Schlieren images of H_2-O_2-CO_2 flame fronts at Φ = 1 and P_i = 1 bar.

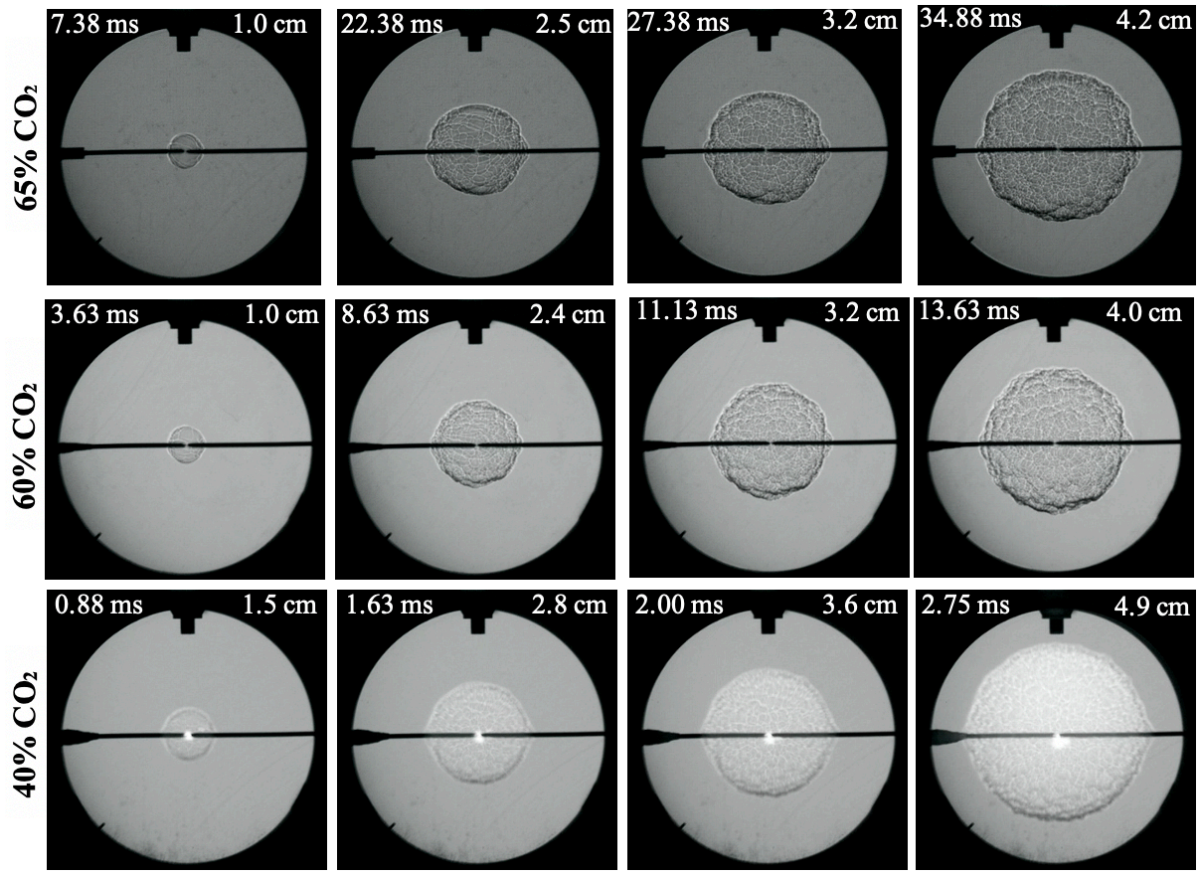

Figure 3: Schlieren images of H_2-O_2-CO_2 flame fronts at Φ = 1 and P_i = 2 bar.

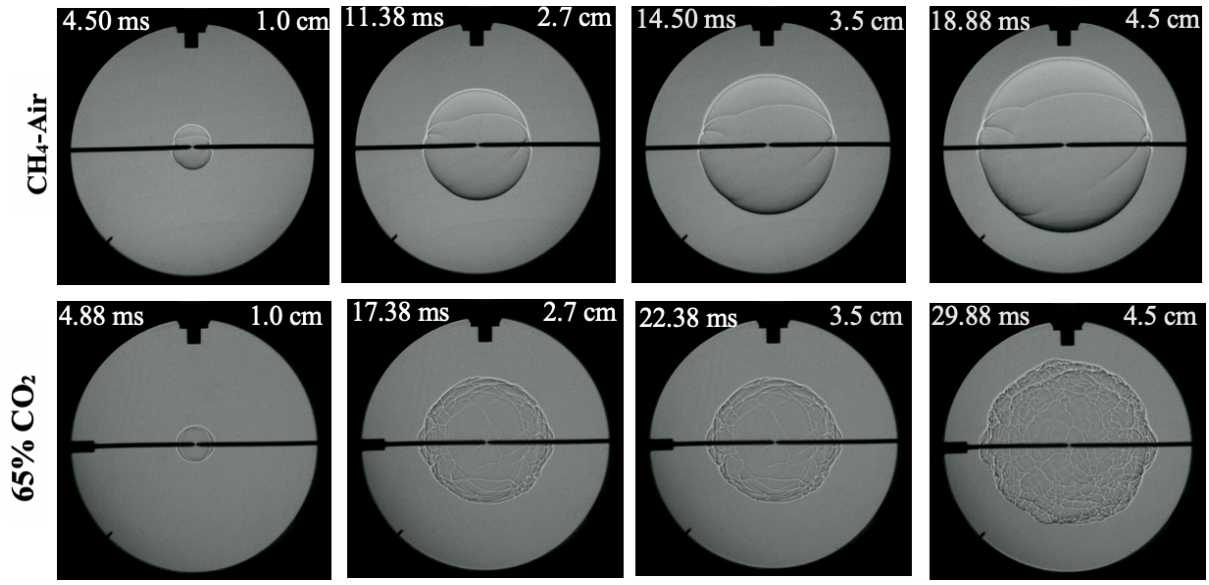

Figure 4: Schlieren images of H_2-O_2-65% CO_2 and CH_4-O_2-N_2 flame fronts at Φ = 1 and P_i = 1 bar.

3.2 Flame speed and laminar burning velocity from Schlieren imaging method

Figure 5 shows the flame speed versus stretch rate curve for stoichiometric hydrogen oxy-combustion at different CO_2 concentrations (40%, 60%, 65%). The same line generated from the schlieren images for stoichiometric methane-air combustion falling between the H_2-O_2-60%CO_2 and H_2-O_2-65%CO_2 lines prove that reduced flame speed of hydrogen oxy-combustion was achieved by gradually increasing the concentration of CO_2 in the mixture.

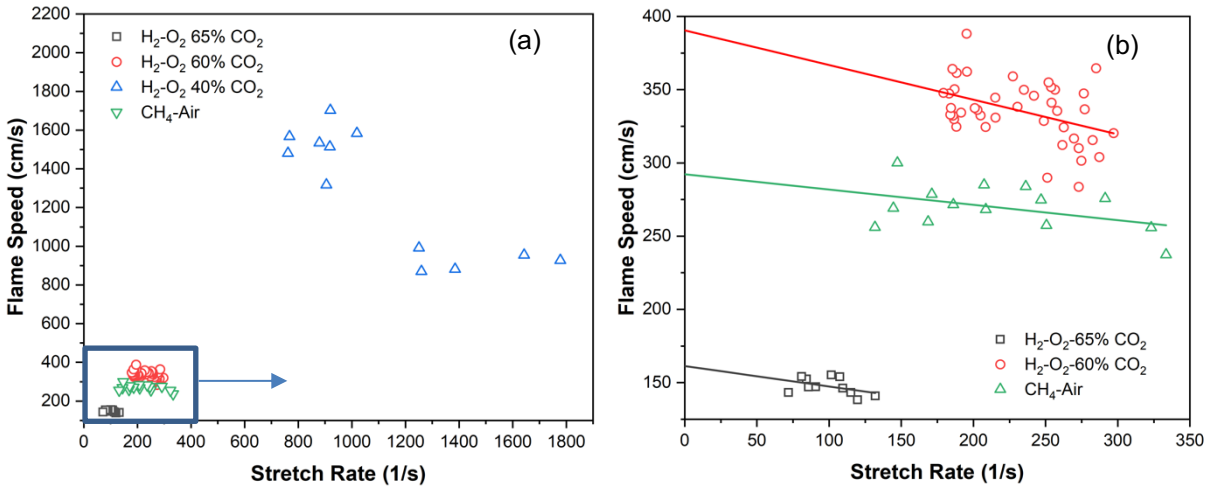

Figure 5: (a) Flame speed vs stretch rate curve for premixed H_2-O_2-65%CO_2, H_2-O_2-60%CO_2, H_2-O_2-40%CO_2 and methane-air combustion at Φ =1 and P_i = 1 bar and (b) linear fit applied to measure the unstretched flame speed.

The unstretched flame speed was calculated by extrapolating these fitted lines for different equivalence ratios at initial pressures of 1 and 2 bar. The average unstretched flame speed was utilized to calculate the laminar burning velocity for these conditions which is presented in Figure 6. It is evident from this plot that regardless of the initial pressure and CO_2 concentration, the LBV showed a reducing trend from stoichiometric to the flame lean conditions. Both 60% and 65% CO_2 cases exhibited an inverse relation of LBV with initial pressure of the gaseous mixture. This trend was also observed in methane-air combustion [32] at different equivalence ratios.

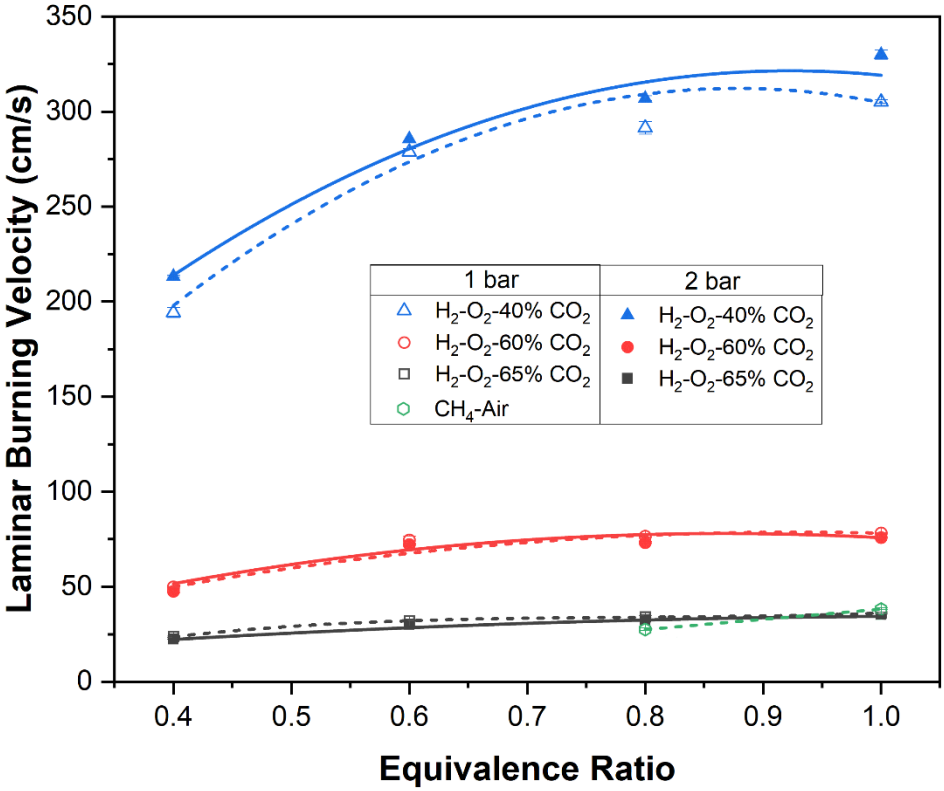

Figure 6: LBV of hydrogen oxy-combustion with CO_2 as the working fluid at different concentrations and equivalence ratios.

An opposite trend was observed for the LBV of H_2-O_2-40% CO_2 combustion where the LBV tends to rise with the increasing initial pressure. This trend matches with the observations made by Ijima and Takeno [33] for hydrogen-air combustion, which indicates that as the CO_2 percentage in the mixture starts to decrease, the data set begins to replicate the conditions seen in standard hydrogen combustion. From the Schlieren images shown in Figures 2 and 3, it is quite evident that at higher pressures, instabilities start to appear quite early in the flame development for H_2-O_2-40%CO_2 combustion. Since these self-accelerating cellular structures, commonly characterized by the Darrieus-Landau instability [35], [36], become more dominant at higher pressures, the flame propagates at a much faster rate.

The sources of error in this method can be classified into two categories: error in mixture preparation and error in data analysis. The first one can be attributed to the purity of the gases used and the accuracy of the pressure transducers in determining the partial pressures of the reactant gasses while filling up the chamber. Since all the gases used in this study had the purity level of 99.999% and the pressure transducer in use had an uncertainty level of ≤ ± 0.3%, this type of error was deemed extremely small and were not presented in Figure 6. The error from data analysis is the compilation of the errors made during the flame radius calculations. These were mitigated by repeating each experiment three times and then applying a linear fit to the flame speed vs stretch rate curve. This error is listed in the Y-axis direction of Figure 6 for each of the cases tested.

3.3 Laminar burning velocity from timed pressure data

Figure 7 shows a positive correlation between the measured laminar burning velocity, S_u from the timed pressure data and the unburned gas temperatures of all the conditions of premixed H_2-O_2-CO_2 combustion experiments. By means of extrapolation, the LBV at 298K can be calculated which can be compared with the measured LBV from the schlieren images.

The LBV has a steeper climb with increasing unburned gas temperatures for cases with 60% CO_2 compared to the 65% cases. Just like the LBV measurements from the schlieren images, the 65% data matches the closest with the stoichiometric methane-air combustion observed by Baghirzade et. al. [32]. It is also interesting to note that the measured LBV from the Schlieren images (Figure 6) turned

out to be almost identical with the extrapolated LBV from the pressure rise method at 298K for 65% cases, whereas the values for 60% cases were slightly lower.

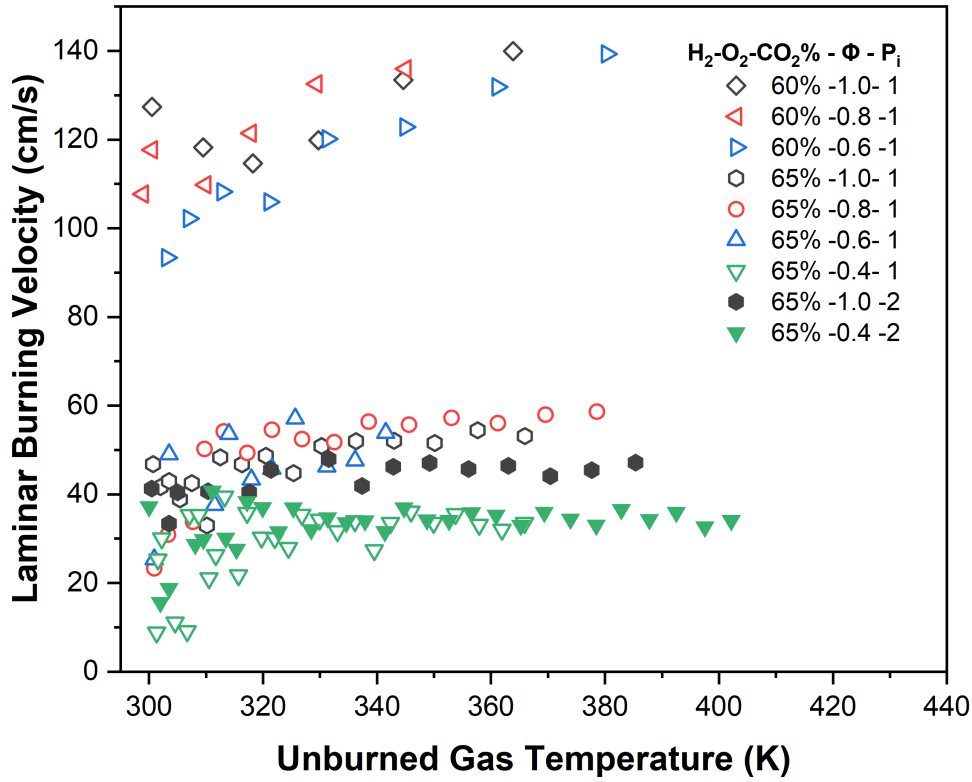

Figure 7: Effect of unburned gas temperature on the laminar burning velocity, S_u, of premixed H_2-O_2-CO_2 combustion experiments at different equivalence ratios and initial pressure

The error in the velocity measurements can be attributed to multiple factors: calibration of the pressure transducers and data analysis errors. Numerical modelling shows that a 1% error in pressure measurements will result in a 1% error in the burning velocity measurements since the fractional pressure rise is not quite proportional to the burned mass fraction [37]. This effect is more dominant in the cases where the CO_2 concentration in lower (60%, 40%), resulting in the measured LBV values from two methods not being identical in the presented 60% CO_2 cases.

3.4 Flammability limit in terms of Maximum CO_2 allowed

The flammability limit of each of the mixture configuration was obtained in accordance with the procedure mentioned in Section 2.3. Table 2 exhibits the maximum allowed percentage of CO_2 as a function of equivalence ratio and initial pressure of the mixture.

Table 2. Maximum Percentage of CO_2 at which ignition occurred for each oxy-combustion equivalence ratio

Φ	*Initial Pressure, P_i (bar)*		
	1	**1.5**	**2**
1	76%	76%	75%
0.8	80%	80%	79%
0.6	82%	82%	82%

The equivalence ratio in Table 2 is that of oxy-combustion, i.e., the ratio of stoichiometric H_2-O_2 to the mixture's H_2-O_2 molar ratio, with the working fluid (CO_2) varied separately as a percentage of the total mixture. Varying the two independently leads to an interesting observation, wherein decreasing the equivalence ratio at a fixed pressure allows for more CO_2 in the mixture before the FL is reached. For example, with Φ = 1 at an initial pressure of 1 bar, the mixture can be up to 76% of CO_2 before it stops

igniting. However, with the same pressure, when the equivalence ratio was decreased to 0.8 and 0.6, the maximum amount of CO_2 which results in ignition was 80% and 82% respectively. This means that more CO_2 can be added to the mixture, despite the fuel being more diluted. There are several factors that could be contributing to this phenomenon. The minimum ignition energy (MIE) is affected by the mixture's properties if all other factors pertaining to the energy source are kept constant. The properties that are relevant to this current case (where only the fraction of the working fluid is changing) include the initial values of the mixture's density (ρ), specific heat at constant pressure (c_p), thermal diffusivity (α), and the associated laminar-flame propagation velocity [38]. C_p and thermal conductivity (k) are greater for H_2 compared to O_2 and CO_2. While both properties have the opposite effect on the thermal diffusivity, the higher density of O_2 and CO_2 means that hydrogen ultimately has a much higher thermal diffusivity. Therefore, as the ratio of hydrogen in the mixture decreases, the effective thermal diffusivity of the mixture becomes low enough to significantly reduce the MIE and allow for the addition of more of the working fluid (CO_2). However, the interplay between these factors could be more complicated and warrants a more detailed investigation. It is also worth noting that the flame at such extremely lean equivalence ratios with higher CO_2 percentages experience a noticeably increased buoyancy as well.

4. Conclusions

The effect of using CO_2 as a working fluid for hydrogen oxy-combustion at different initial pressures and equivalence ratios in an optically accessible CVCC was studied in terms of the flame structure, stretched and unstretched flame speed, laminar burning velocity, and flammability limit. The different observations from all the tested cases can be summarized by the following,

- The highest flame speed and laminar burning velocity was achieved at stoichiometric conditions for all the tested cases (different CO_2 concentrations and initial pressures). The flame speed decreased gradually as the mixture got leaner.
- Increasing the concentration of CO_2 in the mixture lowers the flame speed. After comparing the varying CO_2 concentrated cases, it was shown that the flame speed of the methane-air stoichiometric combustion falls between the unstretched flame speed range for mixtures containing 60% and 65% CO_2.
- At 40% CO_2 concentration, the flame front propagated faster as the initial pressure was increased. The opposite trend was observed for 60% and 65% CO_2, which resembles CH_4-air combustion.
- A positive correlation was seen between the laminar burning velocity and the unburned gas temperature irrespective of equivalence ratio and initial mixture pressure. Furthermore, decreasing the CO_2 percentage in the gaseous mixture resulted in the LBV vs unburned gas temperature curve exhibiting a steeper rise.
- A leaner H_2-O_2 mixture allows for CO_2 in the total mixture, albeit with increased buoyancy.

The inclusion of carbon dioxide as a working fluid in hydrogen oxy-combustion provides the opportunity to achieve flames with LBVs that are appropriate for practical combustion applications. It also eliminates the production of NOx emissions and enables carbon separation or closed-cycle processes. It also opens up opportunities for future studies to pinpoint the mixture configuration where the relation between the LBV and initial mixture pressure inverts. Additional studies will be conducted to determine the parameters that enable the extension of LFL for H_2-O_2-CO_2 combustion as the mixture gets leaner.

References

[1] S. K. Ribeiro, M. J. Figueroa, F. Creutzig, C. Dubeux, J. Hupe, S. Kobayashi, L. A. d. M. Grettas, T. Thrasher, S. Webb and J. Zou, "Chapter 9 - Energy End-Use: Transport," in *Global Energy Assessment - Towards a Sustaiable Future*, Cambridge University Press, 2012, pp. 575 - 648.

[2] S. M. Sarathy, A. Farooq and G. T.Kalghatgi, "Recent progress in gasoline surrogate fuels," *Progress in Energy and Combustion Science,* vol. 65, no. March, pp. 67-108, 2018.

[3] G. Kalghatgi, H. Levinsky and M. Colket, "Future transportation fuels," *Progress in Energy and Combustion Science,* vol. 69, no. November, pp. 103-105, 2018.

[4] G. Kalghatgi, "Is it really the end of internal combustion engines and petroleum in transport?," *Applied Energy,* vol. 225, no. September, pp. 965 - 974, 2018.

[5] OPEC Secretariat, "World Oil Outlook 2045," OPEC, Vienna, 2021.

[6] A. Hula, A. Maguire, A. Bunker, T. Rojeck and S. Harrison, "The 2021 Automotive Trends Report," US Environmental Protection Agency (EPA), 2021.

[7] A. Kumamoto, H. Iseki, R. Ono and T. Oda, "Measurement of minimum ignition energy in hydrogen-oxygen-nitrogen premixed gas by spark discharge," *Journal of Physics: Conference Series,* vol. 301, no. June, p. 012039, 2011.

[8] L. V. Hoecke, L. Laffineur, R. Campe, P. Perreault, S. W. Verbruggen and S. Lenaerts, "Challenges in the use of hydrogen for maritime applications," *Energy and Environmental Science,* vol. 14, no. 2, pp. 815-843, 2021.

[9] J. Lee, J. Kim, J. Park and O. C. Kwon, "Studies on properties of laminar premixed hydrogen-added ammonia/air flames for hydrogen production," *International Journal of Hydrogen Energy,* vol. 35, no. 3, pp. 1054-1064, 2010.

[10] H. Dagdougui, R. Sacile, C. Bersani and A. Ouammi, "Hydrogen Logistics: Safety and Risks Issues," in *Hydrogen Infrastructure for Energy Applications: Production, Storage, Distribution and Safety*, Academic Press (Elsevier), 2018, pp. 127-131.

[11] V. D. Sarli and A. D. Benedetto, "Effects of non-equidiffusion on unsteady propagation of hydrogen-enriched methane/air premixed flames," *International Journal of Hydrogen Energy,* vol. 38, no. 18, pp. 7510-7518, 2013.

[12] L. Qiao, Y.Gu, W. J. A. Dahm, E. S. Oran and G. M. Faeth, "A study of the effects of diluents on near-limit H2–air flames in microgravity at normal and reduced pressures," *Combustion and Flame,* vol. 151, no. 1-2, pp. 196-208, 2007.

[13] L. Qiao, C. H. Kim and G.M.Faeth, "Suppression effects of diluents on laminar premixed hydrogen/oxygen/nitrogen flames," *Combustion and Flame,* vol. 143, no. 1-2, pp. 79-96, 2005.

[14] H. Wei, Z. Xu, L. Zhou, J. Zhao and J. Yu, "Effect of hydrogen-air mixture diluted with argon/nitrogen/carbon dioxide on combustion processes in confined space," *International Journal of Hydrogen Energy,* vol. 43, no. 31, pp. 14798-14805, 2018.

[15] N. F. Munajat, C. Erlich, R. Fakhrai and T. H.Fransson, "Influence of water vapour and tar compound on laminar flame speed of gasified biomass gas," *Applied Energy,* vol. 98, pp. 114-121, 2012.

[16] E. Monteiroa, A. Rouboa, M. Bellenoue, B. Boust and J. Sotton, "Multi-zone modeling and simulation of syngas combustion under laminar conditions," *Applied Energy,* vol. 114, pp. 724-734, 2014.

[17] J.Natarajan, T. Lieuwen and J. Seitzman, "Laminar flame speeds of H2/CO mixtures: Effect of CO2 dilution, preheat temperature, and pressure," *Combustion and Flame,* vol. 151, no. 1-2, pp. 104-119, 2007.

[18] W. Zhang, Z. Chen and W. Kong, "Effects of diluents on the ignition of premixed H2/air mixtures," *Combustion and Flame,* vol. 159, no. 1, pp. 151-160, 2012.

[19] Y. Li, M. Bi, L. Huang, Q. Liu, B. Li, D. Ma and W. Gao, "Hydrogen cloud explosion evaluation under inert gas atmosphere," *Fuel Processing Technology,* vol. 180, pp. 96-104, 2018.

[20] J. Duan and F. Liu, "Laminar combustion characteristics and mechanism of hydrogen/air mixture diluted with N2 + H2O," *International Journal of Hydrogen Energy,* vol. 42, no. 7, pp. 4501-4507, 2017.

[21] M. Morovatiyan, M. Shahsavan, J. Aguilar and J. H. Mack, "Effect of Argon Concentration on Laminar Burning Velocity and Flame Speed of Hydrogen Mixtures in a Constant Volume Combustion Chamber," *Journal of Energy Resources Technology,* vol. 143, no. 3, p. 032301, 2021.

[22] L.-Q. Wang, H.-H. Ma and Z.-W. Shen, "Explosion characteristics of hydrogen-air mixtures diluted with inert gases at sub-atmospheric pressures," *International Journal of Hydrogen Energy,* vol. 44, no. 40, pp. 22527-22536, 2019.

[23] W. Feng, L. Shibo, H. Yizhuo and J. Huiqiao, "The chemical effect of CO2 on the methane laminar flame speed in O2/CO2 atmosphere," *IOP Conference Series: Earth and Environmental Science,* vol. 186, p. 012050, 2018.

[24] A. Ueda, K. Nisida, Y. Matsumura, T. Ichikawa, Y. Nakashimada, T. Endo and W. Kim, "Effects of hydrogen and carbon dioxide on the laminar burning velocities of methane–air mixtures," *Journal of the Energy Institute,* vol. 99, pp. 178-185, 2021.

[25] H.-M. Li, G.-X. Li, Z.-Y. Sun, Z.-H. Zhou, Y. Li and Y. Yuan, "Fundamental combustion characteristics of lean and stoichiometric hydrogen laminar premixed flames diluted with nitrogen or carbon dioxide.," *Journal of Engineering for Gas Turbines and Power,* vol. 138, no. 11, 2016.

[26] T. Katsumi , Y. Yoshida, R. Nakagawa, S. Yazawa, M. Kumada, D. Sato, T. T. Aung, N. Chaumeix and S. Kadowaki, "The effects of addition of carbon dioxide and water vapor on the dynamic behavior of spherically expanding hydrogen/air premixed flames," *Journal of Thermal Science and Technology,* 2021.

[27] N. Ladommatos , S. Abdelhalim, H. Zhao and J. Hu, "The Dillution, Chemical, and ThermEffects of Exhaust Gas Recirculation on Diesel Engine Emissions Parts 2: Effect of Carbon Dioxide," in *Society of Automotive Engineers*, Warrendale, PA, 1996.

[28] N. Ladommatos , S. Abdelhalim, H. Zhao and J. Hu, "The Dillution, Chemical, and Thermal Effects of Exhaust Gas Recirculation on Diesel Engine Emissions Parts 4: Effects of Carbon Dioxide and Water Vapor," in *Society of Automotive Engineers*, Warrendale, PA, 1997.

[29] H. Gossler , S. Drost , S. Porras, R. Schießl, U. Maas and O. Deutschmann, "The internal combustion engine as a CO2 reformer," *Combustion and Flame,* vol. 207, pp. 186-195, 2019.

[30] D. Bradley, P. H. Gaskell and X. J. Gu, "Burning Velocities, Markstein Lengths, and Flame Quenching for Spherical Methane-Air Flames: A Computational Study," *Combustion and Flame,* vol. 104, pp. 176-198, 1996.

[31] M. Metghalchi and J. C. Keck, "Burning velocities of mixtures of air with methanol, isooctane, and indolene at high pressure and temperature," *Combustion and Flame ,* vol. 48, p. 191–210, 1982.

[32] M. Baghirzade, M. N. Nasim, B. Nawaz, J. Aguilar, M. Shahsavan, M. Morovatiyan and J. H. Mack, "Analysis of Premixed Laminar Combustion of Methane With Noble Gases as a Working Fluid," in *ASME 2021 Internal Combustion Engine Division Fall Technical Conference*, 2021.

[33] T. Iijima and T. Takeno, "Effects of temperature and pressure on burning velocity," *Combustion and Flame,* vol. 65, no. 1, pp. 35-43, 1986.

[34] W. Feng, L. Shibo, H. Yizhuo and J. Huiqiao, "The chemical effect of CO2 on the methane laminar flame speed in O2/CO2 atmosphere," *IOP Conference Series: Earth and Environmental Science,* vol. 186, no. 2, 2018.

[35] W. Kim, Y. Sato, T. Johzaki, T. Endo, D. Shimokuri and A. Miyoshi, "Experimental study on self-acceleration in expanding spherical hydrogen-air flames," *International Journal of Hydrogen Energy,* vol. 43, no. 27, pp. 12556-12564, 2018.

[36] C. Bauwens, J. Bergthorson and S. Dorofeev, "Experimental investigation of spherical-flame acceleration in lean hydrogen-air mixtures," *International Journal of Hydrogen Energy,* vol. 42, no. 11, pp. 7691-7697, 2017.

[37] N. Hinton, R. Stone and R. Cracknell, "Laminar burning velocity measurements in constant volume vessels– Reconciliation of flame front imaging and pressure rise methods," *Fuel,* pp. 446-457, 2018.

[38] V. Kurdyumov, J. Blasco, A. Sánchez and A. Liñán, "On the calculation of the minimum ignition energy," *Combustion and Flame,* vol. 136, no. 3, pp. 394-397, 2004.